Thermally stimulated tunneling in rare-earth-doped oxyorthosilicates

A. Vedda,[1,*] M. Nikl,[1,2] M. Fasoli,[1] E. Mihokova,[2] J. Pejchal,[2] M. Dusek,[2] G. Ren,[3] C. R. Stanek,[4] K. J. McClellan,[4] and D. D. Byler[4]

[1]*Department of Materials Science, University of Milano-Bicocca, Via Cozzi 53, 20125 Milan, Italy*

[2]*Institute of Physics, AS CR, Cukrovarnicka 10, 162 53 Prague, Czech Republic*

[3]*Shanghai Institute of Ceramics (SIC), 200050 Shanghai, China*

[4]*Los Alamos National Laboratory, Los Alamos, New Mexico 87545, USA*

(Received 19 May 2008; revised manuscript received 31 October 2008; published 25 November 2008)

We present an investigation of defects acting as electron traps in Lu_2SiO_5 (LSO) and $Lu_xY_{2-x}SiO_5$ (LYSO) performed by wavelength-resolved thermally stimulated luminescence (TSL) measurements from 20 to 400 °C after room-temperature (RT) x-ray irradiation. Single crystals doped with several rare-earth ions such as Ce, Tb, Tm, and Sm were considered. A comparison between TSL and RT radio-luminescence (RL) emission spectra is also presented. The glow curves for both LSO and LYSO are similar, showing a series of TSL peaks at 78, 135, 181, and 236 °C. In addition, a further peak at about 300 °C is observed only in LYSO. Our results confirm the role of oxygen vacancies as electron traps in the material; the presence of several glow peaks with a unique trap depth (0.99 eV ± 0.07 eV) for the 78, 135, 181, and 236 °C peaks is explained by suggesting that electrons stored in oxygen vacancies recombine through a thermally assisted tunneling mechanism with holes localized at Ce^{3+} or Tb^{3+} centers residing on Lu sites at different crystallographic distances from the traps. This model is supported by the very good correlation among O-Lu distances in the monoclinic $C2/c$ structure of LSO and LYSO and the frequency factors of the traps containing the transmission coefficients of the potential barriers between traps and centers, evaluated in the framework of the thermally assisted tunneling process. Tm and Sm ions do not act as TSL recombination centers possibly due to their tendency to trap electrons during irradiation with ionizing radiation.

DOI: 10.1103/PhysRevB.78.195123 PACS number(s): 78.60.Kn, 61.72.J−, 72.20.Jv

I. INTRODUCTION

Ce-doped oxyorthosilicate single crystals have already been candidates for scintillator applications 25 years ago,[1] but systematic research has only increased in the past few years after a particularly promising compound, namely, Lu_2SiO_5:Ce (LSO:Ce), was identified.[2] A preferable combination of high density (7.4 g/cm^3), high light yield (~30 000 photons/MeV), and fast scintillation decay governed by the 40–45 ns decay time, just slightly longer with respect to the photoluminescence one of the Ce^{3+} center (35 ns), was found in LSO:Ce. Additionally, the scintillation emission is favorably placed in the violet region of the spectrum. Among the drawbacks are a worse-than-expected energy resolution of 7.75% (Ref. 3) and an expensive and demanding synthesis procedure (Czochralski crystal-growth method requiring an iridium crucible) due to the high melting point (~2150 °C) of this compound.[4,5] The mentioned advantages further combined with the mechanical and chemical stabilities of the oxide structure led to the introduction of this material in commercial applications, especially in the medical imaging field,[6] after solving the initial problems concerning crystal growth and reproducibility.[3] Later, the yttrium-admixed (5%–10% of total Lu+Y content) LSO [$Lu_xY_{2-x}SiO_5$ (LYSO)] host was also proposed,[7] which seems to be even more advantageous due to less problematic crystal growth and a more favorable Ce segregation coefficient, even though the structure and scintillation mechanisms in both LSO and LYSO are analogous.[8,9] An apparent advantage of LSO:Ce with respect to aluminum perovskite and garnet scintillators consists in the lower concentration of shallow traps which delay the radiative recombination at Ce^{3+} emission centers in the scintillation mechanism and which are responsible for slow scintillation decay components and light yield decrease in the latter materials. This fact is proved by a comparably lower thermally stimulated luminescence (TSL) signal observed below room temperature (RT).[10,11] Nonradiative losses can occur due to the existence of two cerium centers as Ce^{3+} is substituting to both lutetium sites in LSO structure,[12] and at one of them (Lu2 with six oxygen neighbors) the Ce^{3+} emission is quenched above 80 K.[2] However, the scintillation efficiency decrease due to this fact should not be dramatic since it was found by EPR and Raman measurements that the relative occupancy of the Ce2 site is about 5%–10%.[9,13]

In the study of energy transfer and storage processes in the scintillation mechanism of LSO:Ce and LYSO:Ce, a considerable and pronounced sample-dependent afterglow at RT was noticed.[14] TSL measurements above RT were reported also by other groups,[15–17] and oxygen vacancies were proposed as possible electron traps. As many as six peaks were observed in the glow curve above RT. Their spectral emission coincides with Ce^{3+} $5d$-$4f$ transition; the related trap depths were calculated to be about 1 eV even if some differences in values were reported in different studies. The presence of oxygen vacancies was also studied by means of theoretical calculations which revealed that the vacancy related to the Si-unbound oxygen site should be energetically more favorable with respect to other oxygen sites.[18]

The aim of this paper is to provide a more detailed explanation of the recombination mechanism between electrons and holes localized at deep electron traps and Ce^{3+} ions, respectively. For this purpose, wavelength-resolved TSL

studies from 20 to 400 °C were performed and coupled with radio-luminescence (RL) and phosphorescence measurements on LSO and LYSO single crystals. For LSO, different rare-earth ion dopants such as and Ce, Tb, Sm, and Tm were also considered. The results are interpreted, taking into account a thermally assisted tunneling process between oxygen vacancy electron traps and rare-earth ion recombination centers.

II. EXPERIMENTAL CONDITIONS

The investigated samples were single crystals grown in two different institutions. Lu_2SiO_5:0.5 mol % Ce (LSO:Ce) and $Lu_{1.96}Y_{0.04}SiO_5$:0.5 mol % Ce (LYSO:Ce) grown by Czochralski technique with 99.95% purity starting materials were prepared at the Shanghai Institute of Ceramics (SIC), Shanghai, China. Undoped LSO, as well as LSO doped with Ce, Tb, Tm, and Sm with concentrations in the melt of 0.2 at. % with respect to rare-earth elements, were grown by the Czochralski technique at the Los Alamos National Laboratory, Los Alamos, USA. All Starting rare-earth oxide powders were at least 99.99% pure with respect to other rare-earth elements. True dopant concentrations in these crystals were evaluated by x-ray electron probe microanalysis (JEOL JXA 733), and they turned out to be 0.04 at. % for Ce, 0.19 at. % for Tb, 0.20 at. % for Tm, and 0.12 at. % for Sm. The concentrations of Ce^{3+} and Tb^{3+} present as trace impurities in Ce or Tb nondoped samples were evaluated by comparing their room-temperature optical absorption spectra with those of Ce- and Tb-doped crystals featuring Ce^{3+} $4f$-$5d$ and Tb^{3+} $4f$-$4f$ transitions and were less than 1 ppm in all cases. From an analogous comparison, the Ce concentration in Ce-doped crystals from SIC was 0.30–0.40 at. %. The crystals were cut into $7\times7\times1$ mm^3 samples, and the surfaces were polished to an optical grade.

TSL measurements after RT x-ray irradiation (by a Machlett OEG 50 x-ray tube operated at 20 kV) were performed from RT up to 400 °C with a linear heating rate of 1 °C/s using two different apparatuses. The first apparatus used was a homemade high sensitivity TSL spectrometer measuring the TSL intensity as a function of both temperature and emission wavelength; the detector was a double stage microchannel plate followed by a 512 diode array; the dispersive element was a 140 lines/mm holographic grating, the detection range being 200–800 nm. In the second TSL apparatus the total emitted light was detected as a function of temperature by photon counting using an EMI 9635 QB photomultiplier tube. The spectral resolution was approximately 15 nm; in some cases, TSL glow curves were corrected for the temperature dependence (TD) of the $5d_1$-$4f$ radiative transition of Ce^{3+}.

RT radio-luminescence spectra were recorded under continuous x-ray excitation with a Philips 2274 x-ray source (operated at 20 kV) using a monochromator (Triax Jobin-Yvon) coupled to a Jobin-Yvon Spectrum One charge-coupled device (CCD). In this case the detection range was 200–1050 nm and the spectral resolution was 5 nm. The same experimental setup also allowed to perform phosphorescence measurements at RT, lasting 30 s just after the end of irradiation.

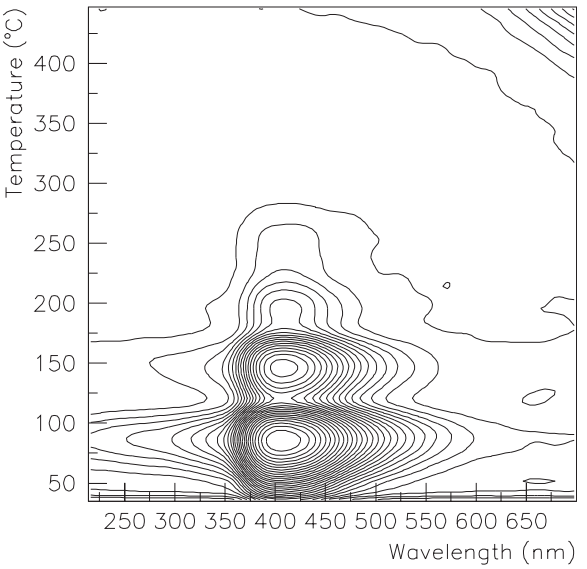

FIG. 1. Contour plot of a wavelength-resolved TSL measurement performed on LSO:Ce following x-ray irradiation at RT. Heating rate=1 °C/s.

Measurements of PL characteristics were performed from 295 to 500 K using a liquid nitrogen bath optical cryostat (Oxford Instruments) working in the 80–500 K range. A 199S spectrofluorometer (Edinburgh Instruments) was used. A single grating emission monochromator and Peltier-cooled TBX-04 detection module (IBH, Scotland) working in photon counting mode were used for the detection. Emission spectra were measured in steady-state and time-resolved mode (0–500 ns time gate) using a steady-state hydrogen lamp and a nanosecond-pulsed hydrogen-filled flashlamp as the excitation sources, respectively. The measured spectra were corrected for the spectral response of the detection system (emission monochromator with TBX-04 detection module).

III. RESULTS AND DISCUSSION

A. Glow peaks and recombination centers

Wavelength-resolved TSL measurements from 20 to 400 °C were performed for all samples; the contour plot of the TSL measurement of LSO:Ce is presented in Fig. 1 as an example. It features several peaks up to 250 °C with an emission spectrum characteristic of the $5d_1$-$4f$ transition of Ce^{3+} at 410 nm (3.02 eV), clearly revealing the role of this dopant as recombination center. The long wavelength emission above 300 °C is due to the blackbody radiation of the system. Moreover, information concerning the shape and temperature position of glow peaks was also obtained by TSL measurements performed in a classical TSL apparatus where light was collected with a photomultiplier. Figure 2 displays data for LSO:Ce and for LYSO:Ce. The curves are similar for both samples; they show a series of TSL peaks, namely, at 78, 135, 181, and 236 °C. In addition, a further peak at about 300 °C is observed only in LYSO:Ce. No variation in glow peak temperature positions was observed

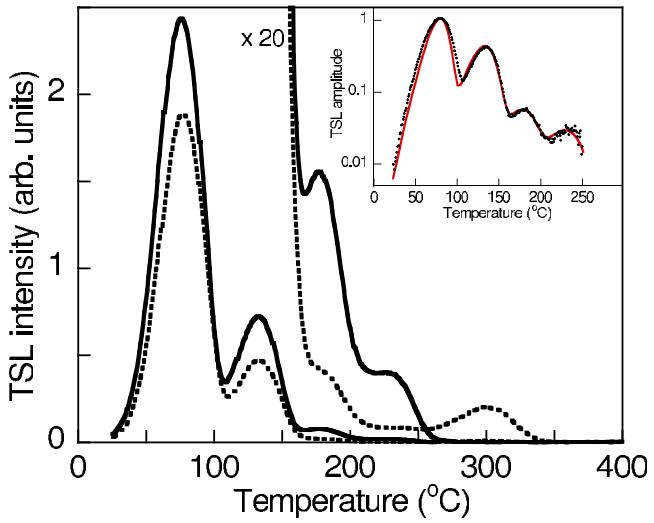

FIG. 2. (Color online) TSL glow curves of LSO:Ce (continuous line) and of LYSO:Ce (dashed line) following x-ray irradiation at RT. Heating rate=1 °C/s. The inset shows the glow curve of LSO:Ce (full circles) corrected for the thermal decay of the Ce^{3+} $5d$-$4f$ transition, together with its numerical reconstruction (continuous red line) in the framework of first-order kinetics. The parameters of the fit are the following ones: E_1=0.97 eV, where $s_1 \sim 10^{13}$ s^{-1}; E_2=0.97 eV, where $s_2 \sim 10^{11}$ s^{-1}; E_3=0.96 eV, where $s_3 \sim 10^9$ s^{-1}; and E_4=0.96 eV, where $s_4 \sim 10^{13}$ s^{-1}.

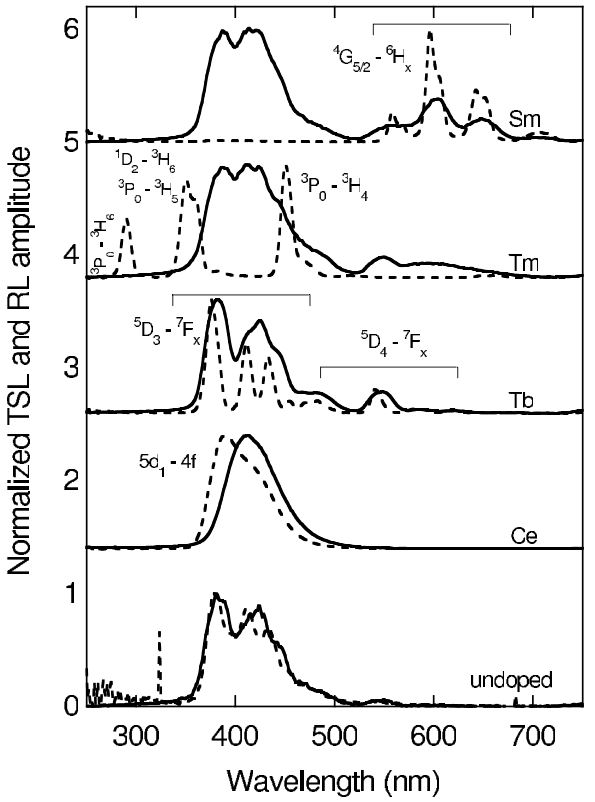

FIG. 3. Room-temperature RL (dashed lines) and TSL (continuous lines) emission spectra of LSO samples doped with different rare-earth ions. The TSL spectra were obtained by integration of wavelength-resolved TSL measurements in the 50–300 °C temperature region.

by varying the irradiation dose (and thus the TSL signal intensity) by more than 2 orders of magnitude, suggesting that the recombination process corresponding to each peak follows first-order kinetics. The glow curves have a general similarity with those observed previously,[14–16] though the peaks above 250 °C were clearly also detected in LSO:Ce.[14,15]

Wavelength-resolved data provide important information regarding the nature of traps involved in the TSL process. In fact, since during ionizing irradiation Ce^{3+} ions are expected to trap holes (temporarily becoming Ce^{4+}) and thus act as hole centers, according to a classical TSL picture defects responsible for TSL traps should have an electronic nature; i.e., they should act as electron traps. The TSL recombination process should be the following:

$$\begin{aligned} &Ce^{4+} + e(\text{freed from the electron trap}) \\ &\rightarrow Ce^{3+*}(\text{excited state}) \rightarrow Ce^{3+} \\ &+ h\nu(\text{TSL emitted light}). \end{aligned} \quad (1)$$

Interesting results confirming the electronic nature of traps were also found by considering, together with Ce-doped crystals, LSO samples doped with other rare-earth ions such as Tb, Tm, and Sm and an undoped sample. Glow curves very similar to those observed in Ce-doped LSO and LYSO were obtained, but they are not reported for the sake of brevity. In Fig. 3 we report the TSL emission spectra obtained by integration of the glow curves from 50 to 300 °C, together with the RL spectra of the same samples measured at RT. We remark that Ce- and Tb-doped crystals have TSL spectra similar to RL ones. The slight shift between RL and TSL spectra in the case of Ce doping might be an instrumental effect; alternatively, it could be due to the involvement, in TSL, of Ce ions close to point defects (electronic traps) giving rise to a different surrounding affecting the position of $5d$-$4f$ transition. A close similarity between TSL and RL spectra occurs also for the undoped sample, where the composite emission in the 360–560 nm range is most probably composed by the spectra of both Ce^{3+} and Tb^{3+} present as trace impurities even if in very low concentration. Significant differences occur for the other dopants: while Tm^{3+} and Sm^{3+} $4f$-$4f$ lines dominate RL spectra of the corresponding doped samples, no clear presence of Tm^{3+} emission is evidenced from the TSL emission spectrum, which is rather characterized by a broad and composite emission similar to that of the undoped crystal (mix of Ce^{3+} and Tb^{3+} spectra). A similar situation is observed for Sm-doped sample. Even if in this case Sm^{3+} lines are also detected at 600 and 650 nm, their intensities are comparable to that of the broad 360–560 nm structure in spite of the much higher content of Sm with respect to Tb and Ce (see Sec. II). Such results demonstrate that different recombination mechanisms occur during RL and TSL; in the latter case the nature of trapped carriers (whether electrons or holes) freed during heating and undergoing radiative recombination selects the dominant recombination centers which appear in the TSL spectrum. The electronic nature of trapped charges responsible for the investigated glow peaks is here well evidenced. The differ-

ences between RL and TSL spectra can be interpreted by considering that, due to their electronic configuration, both Tm^{3+} and Sm^{3+} ions trap preferably electrons during irradiation (becoming temporarily divalent) and thus cannot act as partners in the TSL recombination process with electrons freed from the investigated electron traps. This phenomenon is of course different from that of Ce^{3+} and Tb^{3+}, which will not form divalent cations. Because the TSL glow curves of the Tm- and Sm-doped samples do not show any essential differences, the related electron traps (becoming temporarily Tm^{2+} and Sm^{2+}) should have thermal depths not suitable for identification in the investigated temperature regime. Therefore, TSL recombination in these samples must still involve the few Ce and Tb ions present as trace impurities in very low concentration. This is reflected by the intensities of the glow curves of these samples, which are at least 2 orders of magnitude lower with respect to those of Ce- and Tb-doped crystals for the same irradiation conditions. Moreover, such a difference in the emission spectra between prompt and delayed (i.e., governed by traps) recombinations is also evident in phosphorescence measurements performed at RT immediately after irradiation. Finally, the rather weak Sm^{3+} emission in Sm-doped LSO could be due to an energy-transfer mechanism involving partial reabsorption of Tb^{3+} and Ce^{3+} emissions by Sm^{3+} $4f$ levels in the 20.000–30.000 cm^{-1} range followed by nonradiative de-excitation to the $^4G_{5/2}$ state and by radiative transitions to ^6H_j ground levels.

B. Trap-to-center recombination mechanism

In this section, the trap depths of the TSL peaks and the kind of recombination mechanism are addressed by considering especially Ce-doped crystals. To this purpose, first of all we investigated the TD of the $5d_1$-$4f$ transition of Ce^{3+} responsible for the TSL emission in order to correct the TSL glow curves accordingly.

Such a correction was already applied in two previous papers.[14,15] In the latter one the temperature dependence data reported in Ref. 19 were used. In Ref. 14, the correction curve was constructed based on the TD of nanosecond decay times of Ce^{3+} emission; in Ref. 19 nearly coincident TD curves for emission intensities and nanosecond decay times are reported. The thermal ionization of the $5d_1$ excited state of Ce^{3+} was evidenced by photoconductivity measurement[20] with an onset around RT. The ionization process leads to the nanosecond decay time shortening as it occurs from the relaxed $5d_1$ state. However, electrons are promoted to the conduction band. Such electrons can still radiatively recombine with Ce^{4+} hole centers at later times (and contribute to the luminescence output) in contrast to a classical nonradiative quenching process ending at the Ce^{3+} ground state. To correct our TSL results for the temperature dependence of Ce^{3+} emission intensity and to discuss the approach of the correction construction, we performed the measurements of Ce^{3+} emission spectra in LSO and LYSO hosts above RT up to 500 K (instrumental limit of the 199S machine) in the steady-state and time-resolved (0–500 ns time gate) modes. In Fig. 4 we display the temperature dependence of the integrated emission spectra normalized to 1 at RT. Steady-state

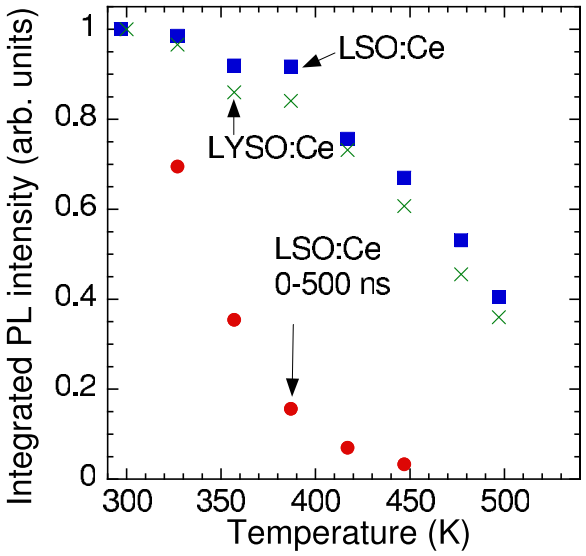

FIG. 4. (Color online) Temperature dependence of the integrated steady-state PL spectra for LSO:Ce and LYSO:Ce samples from SIC, China (filled squares and crosses) and that of integrated time-resolved PL emission spectra (filled circles; emission collected within 0–500 ns after nanosecond pulse excitation) of LSO:Ce. λ_{exc}=355 nm.

integrated spectra show a rather mild decrease above 380 K since the relative intensity at 500 K is about 0.4 with respect to RT. In contrast, the time-resolved integrated emission spectrum decreases much more sharply. Such a difference can be explained by a thermally induced escape of electrons from the relaxed $5d_1$ state of Ce^{3+} to the conduction band and their radiative recombination at Ce^{4+} centers at later times (after 500 ns gate end). Apparently, the delayed recombination of electrons released into the conduction band from the $5d_1$ state of excited Ce^{3+} centers with the Ce^{4+} centers left behind is responsible for the much higher emission intensity in the steady-state detection mode. This is perfectly consistent with the $5d_1$ state ionization above RT evidenced by photoconductivity measurements.[20]

To correct the TSL measurement for the TD of Ce^{3+} emission intensity, one has to consider the steady-state (rather than time-resolved) TD from Fig. 4 due to the steady-state mode of the detector used which allows the detection of both the prompt and delayed recombination processes occurring in the nanosecond and millisecond time scales, respectively.[21] From this point of view the correction curves applied in Refs. 14 and 15 are probably not appropriate as they are closer to that of time-resolved spectra integral in Fig. 4. In fact, the reported relative emission intensities at 400 K with respect to RT are 0.11 in Fig. 4, 0.23 in Ref. 14, and 0.21 in Ref. 15. In the case of the present TSL measurements one can even consider the measured steady-state TDs in Fig. 4 as an upper limit of the temperature quenching of Ce^{3+} emission due to the following reason: in PL measurements electrons thermally released from the $5d_1$ state into the CB can escape from parent Ce^{4+}, migrate in the CB, and get stored/lost in any kind of deep electron trap in the crystal before reaching other Ce^{4+} hole centers. In the present TSL process, however, electrons which escape from Ce^{3+} ions are

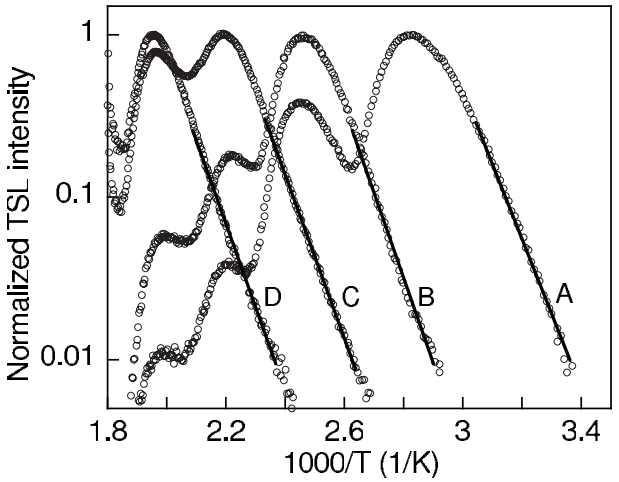

FIG. 5. Arrhenius plots of the TSL of LSO:Ce following x-ray irradiation at RT and partial cleaning at different T_{stop} temperatures. Curve A, 65 °C; curve B, 130 °C; curve C, 175 °C; and curve D, 240 °C. The curves are corrected for the thermal decay of Ce^{3+} emission and normalized to their maximum. Continuous lines are fit of the data according to a single exponential function.

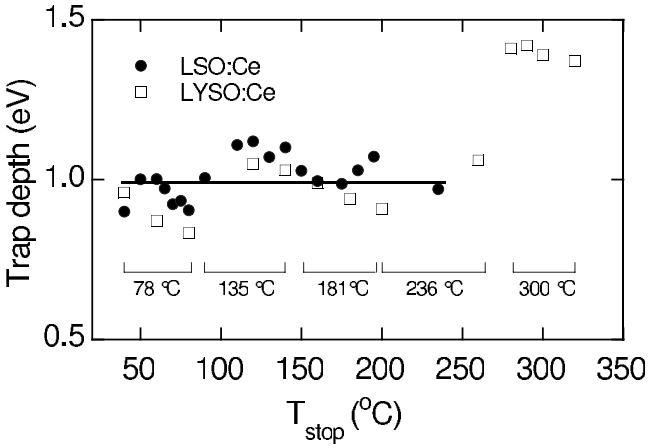

FIG. 6. Trap depths of LSO:Ce and LYSO:Ce evaluated with the initial rise method as a function of T_{stop} temperature. The T_{stop} regions concerning the different glow peaks are marked.

spatially correlated with oxygen vacancies nearby (see further). Such electrons can be easily retrapped by such oxygen vacancies and tunnel again to the same Ce^{4+}; this means that the probability for them to migrate elsewhere and eventually get lost for the TSL radiative recombination process is smaller.

The thermal depth of electron traps was investigated by partial-cleaning TSL measurements followed by the analysis of glow curves with the initial rise method.[22] LSO:Ce and LYSO:Ce samples were first irradiated at RT, then heated at a fixed temperature (T_{stop}), cooled to RT again, and further heated up to 400 °C to record the glow curve. In each case, the trap depth could be evaluated by the fit of the initial portion of the glow curve with the following relation:

$$I(T) = n_0 s \exp\left(\frac{-E}{kT}\right), \tag{2}$$

where n_0 is the initial number of trapped electrons after irradiation, s is the frequency factor, E is the trap depth, k is Boltzmann's constant, and T is the absolute temperature. The Arrhenius plots of selected measurements of LSO:Ce with partial cleanings at 65, 130, 175, and 240 °C are reported in Fig. 5 where the exponential fits are also displayed. Figure 6 reports the trap depth values obtained for all partial cleanings performed on both LSO:Ce and LYSO:Ce in the 40–320 °C extended temperature range; a constant value of $E = 0.99 \pm 0.07$ eV was obtained, which is thus representative of the thermal depths of the whole series of peaks at 78, 135, 181, and 236 °C. The 0.99 eV energy value is similar to those evaluated elsewhere[14] even if in this previous work a constant trap depth was not really evidenced. A significantly different and higher energy (1.4 eV) is found for the highest-temperature peak detected at 300 °C only in LYSO:Ce. However we remark that TSL curves were not corrected above 250 °C for the TD of Ce^{3+} emission so that the true energy value of the 300 °C peak could be slightly higher.

Based on these experimental results, we suggest the occurrence of a thermally stimulated tunneling recombination process between electrons stored in traps and holes stored in hole centers (Ce ions at Lu sites) in order to explain the existence of a common trap depth relative to different glow peaks. In this framework, a single trap can give rise to different glow peaks according to its distance to the recombination center.

In fact, according to first-order recombination process, the temperature maximum T_m of a peak is related to the trap depth E, to the frequency factor s, and to the heating rate β by the following relation:[22]

$$\frac{\beta E}{kT_m^2} = s \exp\left(\frac{-E}{kT_m}\right). \tag{3}$$

For a thermally assisted tunneling process, the trap depth E represents the energy difference between the ground level of the trap and the thermally reached excited level from which electrons tunnel toward the recombination center. The physical meaning of the frequency factor s, which is often disregarded, must be considered in this process. It can be expressed as[23]

$$s = x\nu_T \exp\left(\frac{\Delta S}{k}\right), \tag{4}$$

where x is the transmission coefficient of the barrier, ν_t is the thermal vibration frequency, and $\Delta S/k$ is an entropy factor. The transmission coefficient x takes the form[22]

$$x = \exp(-\varphi r), \tag{5}$$

where ϕ is a constant and r is the trap-to-center distance. So, according to Eqs. (3)–(5), in a thermally stimulated tunneling process the frequency factor s depends exponentially on the trap-to-center distance r, thereby justifying the presence of several glow peaks produced by a single trap located at different discrete distances with respect to the recombination center. This type of recombination mechanism does not im-

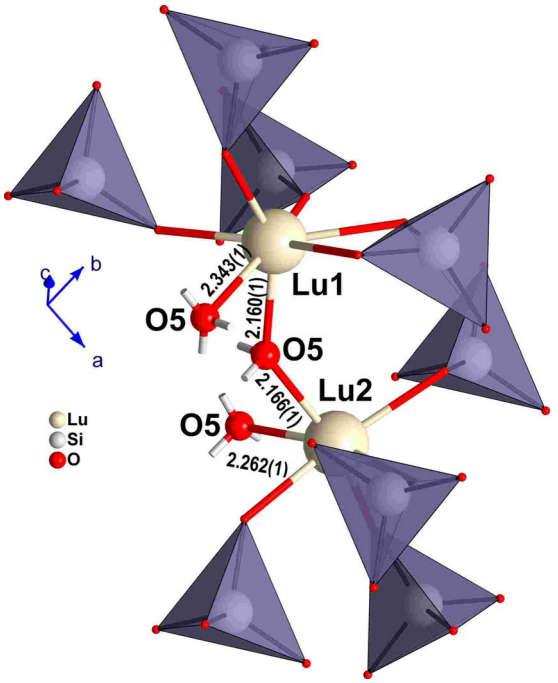

FIG. 7. (Color online) Crystallographic structure of LSO showing two Lu sites (Lu1 and Lu2), Si-unbound oxygen, and surrounding SiO_4 tetrahedra.

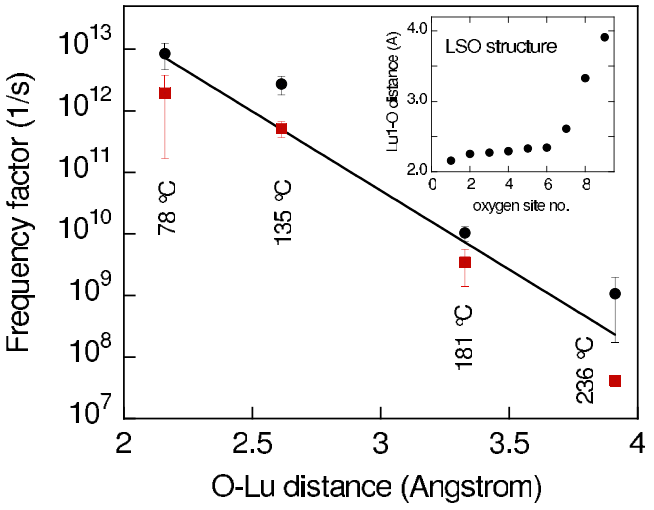

FIG. 8. (Color online) Frequency factors of peaks at 78, 135, 181, and 236 °C vs O-Lu_1 distance in LSO (full circles) and in LYSO (full squares). The continuous line is the exponential fit of all the data. The inset displays the nine nearest O-Lu_1 distances.

ply any thermal carrier delocalization in the conduction band prior to radiative recombination.

To analyze this process more completely, we first make the assumption that oxygen vacancies act as electron traps in the material and are responsible for the investigated glow peaks. This assumption is reasonable because the presence of oxygen vacancies in LSO and their involvement in TSL have already been thoroughly examined in the literature. It was first reported that the TSL intensity of LSO:Ce increases following annealing treatments in reducing atmosphere,[15] and subsequently the role of oxygen vacancies acting as TSL traps responsible for glow peaks below and above RT was suggested.[16,24] Very recently, an electron trapped in oxygen vacancy (F^+ center) was evidenced by EPR and related to the first TSL peak observed above RT.[25] To better understand the effect of oxygen vacancies, we must consider the distances between oxygen sites (and oxygen vacancies) and Lu sites, where substitutional Ce dopant ions are incorporated. Between the two unequal low (C_1) symmetry Lu sites, it is expected that the majority of Ce ions will reside on the larger Lu_1 site, which has 6+1 oxygen nearest neighbors.[9,13] This is of course because Ce^{3+} is larger than Lu^{3+} (sixfold-coordinated ionic radii are 1.01 and 0.861 Å, respectively[26]). Moreover, the emission of Ce^{3+} at the Lu_2 site is quenched at RT.[2] Figure 7 illustrates the LSO structure. Oxygen-Lu_1 distances in monoclinic $C2/c$ LSO (and LYSO) were calculated from structural data.[27] In Fig. 8, the frequency factors obtained by Eq. (3) substituting the energies reported in Fig. 6 and the measured T_m of the peaks are plotted versus oxygen-Lu_1 nearest-neighbor distances. Furthermore, the distance associated with the frequency factor of the lowest-T peak at 78 °C is the shortest among the first six very similar distances that differ by less than 0.2 Å from one another. Since this site is related to the Si-unbound oxygen nearest neighbor, vacancy formation could be energetically more favorable than in other oxygen sites.[18] For completeness, the inset of Fig. 8 reports Lu_1 distances considered in the LSO (LYSO) structure. The data reported in Fig. 8 show that with a good approximation, the frequency factor is an exponential function of Lu_1-O distances; we thus consider this result, together with the constant value of the trap depths and with the occurrence of first-order recombination, as experimental proof that TSL recombination below 250 °C in LSO and LYSO is governed by thermally assisted tunneling recombination processes between spatially correlated electrons stored in oxygen vacancies and holes stored in Ce sites. The correctness of our evaluation is also demonstrated by the satisfactory reconstruction of the glow curves with parameters similar to those obtained by the initial rise, as displayed in the inset of Fig. 2 in the case of LSO:Ce. For tunneling to occur, the excited state of the trap thermally reached by the electron should have a similar energy as that of $5d_1$ Ce state. Since the energy positions of $5d$ states of different rare-earth ions in the band gap are similar (as demonstrated in several compounds[28]), the same should apply to the case of Tb^{3+}, where tunneling transfer in the $5d_1$ state should be followed by nonradiative de-excitation to excited $4f$ states and final radiative recombination to $4f$ ground state. The Lu-O distances here considered refer to the perfect lattice and do not take into account any possible distortion due to the presence of Ce ions. However, any variation in such distances in the presence of Ce should be of the order of the difference in the ionic radii between Lu and Ce, which is approximately 0.15 Å (Ref. 26); so, it should not significantly change the dependence on the frequency factors shown in Fig. 8.

Our explanation is valid for the four peaks at 78, 135, 181, and 236 °C but does not apply to the highest-temperature peak at approximately 300 °C observed only in LYSO which should have a different nature. It is possible that this peak is due to the classical thermal escape of elec-

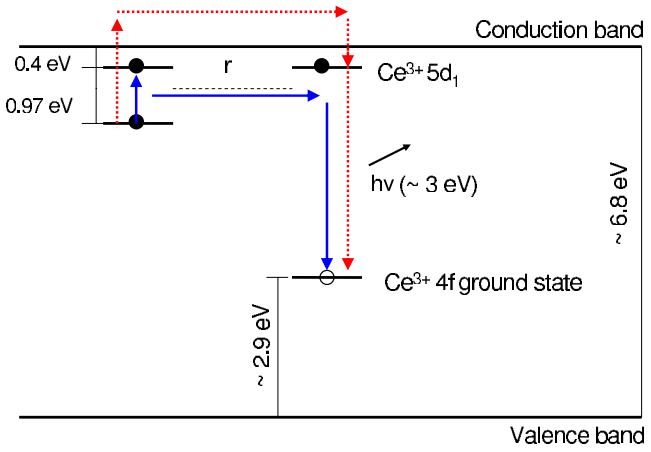

FIG. 9. (Color online) Schematic diagram illustrating the detrapping-recombination processes in LSO and LYSO in the case of Ce doping. In blue (continuous lines), thermally assisted tunneling recombination; in red (dotted lines), detrapping through the conduction band. The position of the $4f$ ground state of Ce^{3+} with respect to the valence band is estimated from literature data (see text).

trons stored in oxygen vacancies into the conduction band, followed by trapping at Ce^{4+} sites and radiative recombination. The probability of this mechanism is supported by the coincidence between the difference in trap depths of this peak and lower-T peaks (0.4 eV), and the thermal ionization energy of the first Ce $5d$ state in LSO as evaluated by photoionization studies.[20] We recall however that TSL curves were not corrected above 250 °C for the TD of Ce^{3+} emission so that the true energy value of the 300 °C peak could be slightly higher. Interestingly, this high-T peak was observed only in LYSO (and not in LSO) so a different nature cannot be excluded. However, the percentage of oxygen vacancies not spatially correlated with Ce ions should be highly dependent on the concentrations of both oxygen vacancies and Ce ions, as well as on growth conditions. Therefore, it is possible that the relative probability of classical thermal escape through the conduction band of the crystal is strongly sample dependent. A schematic representation of the recombination processes for Ce recombination centers operating in LSO and LYSO including thermal escape through the conduction band is presented in Fig. 9: depending on the distance r between oxygen vacancies and Ce ions, different glow peaks can occur (blue path). The escape path through the conduction band is marked red. Considering that the LSO forbidden gap is $E_g \sim 6.5–6.8$ eV (Ref. 29) and that the energy of the $4f$-$5d_1$ absorption transition is 3.5 eV, one can estimate that the position of the Ce^{3+} $4f$ ground state is about 2.6–2.9 eV above the valence band, ensuring the stability of Ce^{4+} (i.e., a hole trapped at a Ce^{3+} ion) as considered in the TSL mechanism. A similar model has been considered in the case of thermostimulated and photostimulated luminescence of Y_2SiO_5:Ce (Ref. 30) where a detailed interpretation of the nature of electron-hole recombination processes was not provided.

Thermally stimulated tunneling recombination processes were already observed and are common in other materials, such as mixed perovskites, ($Lu_xY_{1-x}AlO_3$:Ce),[31] calcite,[32] Zn_2SiO_4:Mn,[33] or RbBr:Tl.[34] The present model is in agreement with general considerations already proposed in the recent literature concerning the existence of a close spatial relation between traps and recombination centers,[14] and of a direct role of metal ion–ligand configurations in tuning the temperature positions in different oxyorthosilicates.[17]

IV. CONCLUSIONS

The nature of traps responsible for afterglow phenomena in LSO and LYSO was addressed by detailed wavelength-resolved TSL measurements above room temperature. We interpret the presence of four glow peaks with the same trap depth as being due to the presence of a single electron trap located at different distances with respect to recombination centers (Ce^{3+} and Tb^{3+} rare-earth dopants); the radiative recombination between electrons and holes occurs through a thermally stimulated tunneling mechanism. We identified oxygen vacancies as the predominant electron trap in LSO and LYSO. The ascription of traps to oxygen vacancies is based on the very good correlation of O-Lu distances (corresponding to distances between oxygen vacancies and substitutional rare-earth ions) in the monoclinic $C2/c$ structure of LSO and LYSO to the frequency factors of the traps which contain the transmission coefficients of the potential barriers between trap and centers.

In summary, our interpretation is grounded on the possibility of explaining the existence of several peaks in the TSL glow curve of a crystal with the same trap depth and different frequency factors by assuming localized recombinations through thermally assisted tunneling. In such process, the parameter that determines the variation in the frequency factors is the trap-to-center distance. The interpretation is supported by (i) the fact that all glow peaks are due to electron traps, evidenced from the comparison between TSL and RL data; (ii) the common nature of the emission centers for all glow peaks; (iii) the similarity of the trap depths of all peaks (E=0.99 eV); and (iv) the exponential dependence of the frequency factors on the oxygen-lutetiun distances (corresponding to the distances between oxygen vacancy traps and cerium recombination centers) as expected in a tunneling process. Our interpretation could be further verified by the extension of similar analyses to other silicates with the $C2/c$ structure such as YSO, YbSO, and ErSO which manifest similar glow curves.[16,17]

TSL experiments can provide a detailed picture about the thermal stability of trapping levels and their recombination processes but are usually not able to provide information about the structural nature of defects responsible for such levels. As we have shown, the situation with LSO and LYSO is one of the very rare cases in which, due to the occurrence of a specific localized recombination mechanism, the TSL technique can also provide insight to the structural nature of traps. Finally, our results provide useful information also from the technological point of view since the reduction in afterglow phenomena could be pursued by a careful control of oxygen vacancy formations during crystal-growth and postgrowth annealing procedures.

ACKNOWLEDGMENTS

The authors gratefully acknowledge the financial support of the Italian Cariplo Foundation Project "Structure and optical properties of self-organized nano- and mesoscopic materials" (2006–2008) and of the Czech projects GA (Contract No. AV IAA100100810) and MSMT KONTAKT (Contract No. ME08034). The authors are grateful to K. Jurek for performing x-ray electron probe microanalysis and to V. Jary for carrying out the photoluminescence experiment and data evaluation.

*Corresponding author. anna.vedda@unimib.it

[1] K. Takagi and T. Fukazawa, Appl. Phys. Lett. **42**, 43 (1983).
[2] H. Suzuki, T. A. Tombrello, C. L. Melcher, and J. S. Schweizer, Nucl. Instrum. Methods Phys. Res. A **320**, 263 (1992).
[3] C. L. Melcher, M. A. Spurrier, L. Eriksson, M. Eriksson, M. Schmand, G. Givens, R. Terry, T. Homant, and R. Nutt, IEEE Trans. Nucl. Sci. **50**, 762 (2003).
[4] T. Utsu and S. Akiyama, J. Cryst. Growth **109**, 385 (1991).
[5] C. L. Melcher, R. A. Manente, C. A. Peterson, and J. S. Schweizer, J. Cryst. Growth **128**, 1001 (1993).
[6] W. W. Moses, Nucl. Instrum. Methods Phys. Res. A **471**, 209 (2001).
[7] D. W. Cooke, K. J. McClellan, B. L. Bennett, J. M. Roper, M. T. Whittaker, R. E. Muenchausen, and R. C. Sze, J. Appl. Phys. **88**, 7360 (2000).
[8] D. Chiriu, N. Faedda, A. G. Lehmann, P. C. Ricci, A. Anedda, S. Desgreniers, and E. Fortin, Phys. Rev. B **76**, 054112 (2007).
[9] P. C. Ricci, C. M. Carbonaro, D. Chiriu, R. Corpino, N. Faedda, M. Marceddu, and A. Anedda, Mater. Sci. Eng., B **146**, 2 (2008).
[10] P. Szupryczynski, C. L. Melcher, M. A. Spurrier, M. P. Maskarinec, A. A. Carey, A. J. Wojtowicz, W. Drozdowski, D. Wisniewski, and R. Nutt, IEEE Trans. Nucl. Sci. **51**, 1103 (2004).
[11] M. Nikl, E. Mihokova, J. Pejchal, A. Vedda, M. Fasoli, I. Fontana, V. V. Laguta, V. Babin, K. Nejezchleb, A. Yoshikawa, H. Ogino, and G. Ren, IEEE Trans. Nucl. Sci. **55**(3), 1035 (2008).
[12] J. Felsche, Struct. Bonding (Berlin) **13**, 99 (1973).
[13] L. Pidol, O. Guillot-Noël, A. Kahn-Harari, B. Viana, D. Pelenc, and D. Gourier, J. Phys. Chem. Solids **67**, 643 (2006).
[14] P. Dorenbos, C. W. W. van Eijk, A. J. J. Bos, and C. L. Melcher, J. Phys.: Condens. Matter **6**, 4167 (1994).
[15] R. Visser, C. L. Melcher, J. S. Schweizer, H. Suzuki, and T. A. Tombrello, IEEE Trans. Nucl. Sci. **41**, 689 (1994).
[16] D. W. Cooke, B. L. Bennett, R. E. Muenchausen, K. J. McClellan, J. M. Roper, and M. T. Whittaker, J. Appl. Phys. **86**, 5308 (1999).
[17] D. W. Cooke, B. L. Bennett, K. J. McClellan, J. M. Roper, and M. T. Whittaker, J. Lumin. **92**, 83 (2001).
[18] B. Liu, Zeming Qi, Mu Gu, Xiaolin Liu, Shiming Huang, and Chen Ni, J. Phys.: Condens. Matter **19**, 436215 (2007).
[19] H. Suzuki, T. Tombrello, C. L. Melcher, and J. S. Schweitzer, IEEE Trans. Nucl. Sci. **40**, 380 (1993).
[20] E. van der Kolk, S. A. Basun, G. F. Imbusch, and W. M. Yen, Appl. Phys. Lett. **83**, 1740 (2003).
[21] M. Nikl, H. Ogino, A. Yoshikawa, E. Mihokova, J. Pejchal, A. Beitlerova, A. Novoselov, and T. Fukuda, Chem. Phys. Lett. **410**, 218 (2005).
[22] S. W. S. Mc Keever, *Thermoluminescence of Solids* (Cambridge University Press, Cambridge, 1985).
[23] D. Curie, *Luminescence in Crystals* (Wiley, New York, 1960).
[24] D. W. Cooke, B. L. Bennett, K. J. McClellan, R. E. Muenchausen, J. R. Tesmer, and C. J. Wetteland, Philos. Mag. B **82**, 1659 (2002).
[25] D. W. Cooke, M. W. Blair, J. F. Smith, B. L. Bennett, L. G. Jacobson, E. A. McKigney, and R. E. Munchausen, IEEE Trans. Nucl. Sci. **55**, 1118 (2008).
[26] R. D. Shannon, Acta Crystallogr. A **32**, 751 (1976).
[27] T. Gustafsson, M. Klintenberg, S. E. Derenzo, M. J. Weber, and J. O. Thomas, Acta Crystallogr. C: Cryst. Struct. Commun. **C57**, 668 (2001).
[28] P. Dorenbos, J. Phys.: Condens. Matter **15**, 8417 (2003).
[29] (a) V. V. Mikhailin, Nucl. Instrum. Methods Phys. Res. A **448**, 461 (2000); (b) Our recent results of intrinsic luminescence vacuum ultraviolet (vuv) excitation spectra at 10 K indicate a band gap close to 6.8 eV.
[30] A. Meijerink, W. J. Schipper, and G. Blasse, J. Phys. D **24**, 997 (1991).
[31] A. Vedda, M. Martini, F. Meinardi, J. Chval, M. Dusek, J. A. Mares, E. Mihokova, and M. Nikl, Phys. Rev. B **61**, 8081 (2000).
[32] R. Visocekas, T. Ceva, C. Marti, F. Lefaucheux, and M. C. Robbert, Phys. Status Solidi A **35**, 315 (1976).
[33] P. Avouris and T. N. Morgan, J. Chem. Phys. **74**, 4347 (1981).
[34] H. von Seggern, A. Meijerink, T. Voigt, and A. Winnacker, J. Appl. Phys. **66**, 4418 (1989).